



This is a repository copy of *Extending the bounds of performance in E-mode p-channel GaN MOSHFETs*.

White Rose Research Online URL for this paper:

<https://eprints.whiterose.ac.uk/119664/>

Version: Accepted Version

Proceedings Paper:

Kumar, A. orcid.org/0000-0002-8288-6401 and De Souza, M.M. (2016) Extending the bounds of performance in E-mode p-channel GaN MOSHFETs. In: 2016 IEEE International Electron Devices Meeting (IEDM). 2016 IEEE International Electron Devices Meeting, 03-07 Dec 2016, San Francisco, CA, USA. IEEE . ISBN 978-1-5090-3901-2

<https://doi.org/10.1109/IEDM.2016.7838368>

© 2017 IEEE. Personal use of this material is permitted. Permission from IEEE must be obtained for all other users, including reprinting/ republishing this material for advertising or promotional purposes, creating new collective works for resale or redistribution to servers or lists, or reuse of any copyrighted components of this work in other works.

Reuse

Items deposited in White Rose Research Online are protected by copyright, with all rights reserved unless indicated otherwise. They may be downloaded and/or printed for private study, or other acts as permitted by national copyright laws. The publisher or other rights holders may allow further reproduction and re-use of the full text version. This is indicated by the licence information on the White Rose Research Online record for the item.

Takedown

If you consider content in White Rose Research Online to be in breach of UK law, please notify us by emailing eprints@whiterose.ac.uk including the URL of the record and the reason for the withdrawal request.



eprints@whiterose.ac.uk
<https://eprints.whiterose.ac.uk/>

Extending the bounds of performance in E-mode p-channel GaN MOSHFETs

A. Kumar¹, and M. M. De Souza¹

¹EEE Department, University of Sheffield, Sheffield, U.K., email: akumar4@sheffield.ac.uk; m.desouza@sheffield.ac.uk

Abstract—An investigation of the distribution of the electric field within a normally-off p-channel heterostructure field-effect transistor in GaN, explains why a high $|V_{th}|$ requires a reduction of the thickness of oxide and the GaN channel layer. The trade-off between on-current $|I_{ON}|$ and $|V_{th}|$, responsible for the poor $|I_{ON}|$ in E-mode devices is overcome with an additional cap AlGaN layer that modulates the electric field in itself and the oxide. A record $|I_{ON}|$ of 50 – 60 mA/mm is achieved with a $|V_{th}|$ greater than $|-2|$ V in the designed E-mode p-channel MOSHFET, which is more than double that in a conventional device.

I. INTRODUCTION

The polarization in hexagonal GaN gives rise to a high density ($> 10^{13} \text{ cm}^{-2}$) electron gas (2DEG) at the interface between AlGaN and GaN. This high mobility, naturally occurring, conducting channel lends itself more easily to high performance depletion mode (D-mode) devices that find applications in high frequency and power. High performance p-channel heterostructure field-effect transistors (p-HFETs) in GaN, utilizing the two dimensional hole gas (2DHG) as carrier, are also highly desirable to enable complementary logic [1], [2] and allow integrated power convertor systems on a chip [3]. Despite the poor mobility of holes in GaN, $\sim 16 \text{ cm}^2/\text{V} \cdot \text{s}$ at room temperature [4], the high density of 2DHG ($\sim 10^{13} \text{ cm}^{-2}$) [5] has resulted in an on-current of $\sim 150 \text{ mA/mm}$ [1] in a normally-on D-mode p-HFET, however, the on/off current ratio I_{ON}/I_{OFF} was only 1.

In contrast, normally-off or enhancement mode (E-mode) p-HFETs with low off-current $|I_{OFF}|$ are desirable to reduce the static power consumption, simplify the circuit complexity, and enable fail-safe operation [6]. However, the on-current, $|I_{ON}|$, for enhancement-mode (E-mode) p-channel HFETs reported to date remains low at 0.1 – 9 mA/mm [1], [2] [7], [8] with a maximum $|V_{th}|$ of $|-1.3|$ V [8], as shown in Fig. 1. One of the widely understood reasons for this behavior is that conditions for increased polarization charge, required to increase $|I_{ON}|$, leads to difficulty in depleting the charge in E-mode, to give low $|I_{OFF}|$, hence leading to poor I_{ON}/I_{OFF} and a low $|V_{th}|$.

In this paper, we first demonstrate that in GaN, achieving a low negative threshold voltage, i.e. high $|V_{th}|$ requires a reduction of the thickness of oxide and GaN channel layers (contrary to well-known behavior of MOSFETs in silicon), which can lead to a significant gate leakage and degradation in the reliability. For the first time, we present the analysis of an alternative heterostructure for E-mode p-channel MOSHFETs in GaN [9] and demonstrate the possibility to “break” the trade-off between $|I_{ON}|$, $|V_{th}|$, and I_{ON}/I_{OFF} in E-mode p-channel

MOSHFETs, that exists even in this modified structure. An analytic model for the V_{th} in terms of thickness of oxide and channel layers (t_{ox} & t_{ch}), and polarization charge σ_p that gives a rule of thumb prediction of the V_{th} is presented.

II. METHODOLOGY

Fig. 2 (a) shows the schematic diagrams of the p-channel MOSHFET with a conventional heterostructure (HS1) and the modified structure (HS2). The hole transport is modelled using the Albrecht mobility model [10] at low field and a nitride specific field dependent mobility at high field [11], as implemented in Silvaco TCAD [12]. The maximum hole mobility at room temperature was limited to $16 \text{ cm}^2/\text{V} \cdot \text{s}$ [4]. With the charge and trap densities of $2.8 \times 10^{12} \text{ cm}^{-2}$ and $2 \times 10^{12} \text{ cm}^{-2}$, respectively at the oxide/GaN channel interface for HS1, our model shows a close match with the experimental results reported in [13] in Fig. 2 (b). The same charge and traps are included in the analysis of the alternate heterostructure HS2.

The threshold voltage equations are derived for both heterostructures HS1 and HS2, using an approach similar to that adopted in [14]:

$$-\frac{\Phi_{1,p}}{e} - V_G + t_{ox}\epsilon_{ox} + t_{ch}\epsilon_{ch} + \frac{\Delta E_{OV}}{e} = \frac{\Delta_p}{e} \geq 0 \quad (1)$$

$$t_b\epsilon_b = \frac{E_G + \Delta_n + \Delta_p}{e} \geq \frac{E_G}{e} \quad (2)$$

$$\sigma_{ox} = \epsilon_{ch}\epsilon_{ch} - \epsilon_{ox}\epsilon_{ox} \quad (3) \quad \sigma_p = \epsilon_{ch}\epsilon_{ch} + \epsilon_b\epsilon_b \quad (4)$$

By eliminating the ϵ_{ox} , ϵ_{ch} , & ϵ_b from above equations:

$$V_G \leq V_{th} \cong \frac{\sigma_p}{C_{oc}} - \frac{\sigma_{ox}}{C_{ox}} - \frac{C_b E_G}{C_{oc} e} - \frac{\Phi_{1,p}}{e} + \frac{\Delta E_{OV}}{e} \quad (5)$$

Where: $C_{ox} = \frac{\epsilon_{ox}}{t_{ox}}$, $C_{ch} = \frac{\epsilon_{ch}}{t_{ch}}$ and $\frac{1}{C_{oc}} = \frac{1}{C_{ox}} + \frac{1}{C_{ch}}$.

A similar analysis can be applied to derive the threshold voltage expression for HS2 in Fig. 2 (a), here we only present the result:

$$V_{th} \cong \frac{\sigma_p}{C_{occ}} - \frac{\sigma_{ox}}{C_{ox}} - \frac{\sigma_{cap}}{C_{ocp}} - \frac{C_b E_G}{C_{occ} e} - \frac{\Phi_{1,p}}{e} + \frac{\Delta E_{OV}}{e} \quad (6)$$

Where $\frac{1}{C_{ocp}} = \frac{1}{C_{ox}} + \frac{1}{C_{cap}}$, and $\frac{1}{C_{occ}} = \frac{1}{C_{ocp}} + \frac{1}{C_{ch}}$, while $C_{cap} = \frac{\epsilon_{cap}}{t_{cap}}$.

Where $\Phi_{1,p}$ is the valence band barrier at gate/oxide interface, ΔE_{OV} is the net valence band offset from oxide to GaN channel, ϵ_i , t_i & \mathcal{E}_i are the permittivity, thickness and electric field for a layer indexed as i , Δ_n & Δ_p are heights of electron and hole quantum wells, and E_G is the band gap of GaN.

III. ANALYSIS OF THE CONVENTIONAL HETEROSTRUCTURE P-CHANNEL MOSHFET (HS1)

A common approach to improve $|I_{ON}|$ in the conventional heterostructure (HS1) in Fig. 2 (a) is to increase the Al mole fraction within the barrier layer x_b . Fig. 3 (a) compares the transfer characteristics of the device at different x_b . An increase in x_b , results in an increase in polarization charge at both the top and bottom AlGaN interfaces, allowing a higher

band bending across the AlGaIn barrier, as shown in Fig. 3 (b). As a result, the energy of the valence band at the top GaN/AlGaIn interface rises, thus facilitating the formation of the hole quantum well, which results in low $|V_{th}|$ and high off-current $|I_{OFF}|$. A fourfold increase in $|I_{ON}|$ is observed at higher x_b , owing to a higher density of the 2DHG, shown in Fig. 3 (c).

An increase in $|V_{th}|$ can be achieved by recessing the GaN layer [8]. In Fig. 4, we examine the dependence of $|V_{th}|$ upon t_{ox} and t_{ch} . A decrease in t_{ox} leads to an improvement in both the I_{ON}/I_{OFF} and $|V_{th}|$, as shown Fig. 4 (a). This is because a smaller t_{ox} lowers the valence band energy relative to the Fermi level at the GaN channel/AlGaIn barrier interface, as shown in Fig. 4 (b). Therefore, a higher $|V_{GS}|$ is now required to increase the valence band energy level for the formation of the 2DHG at this interface. Since the electric field in both oxide and channel layers is pointed along the same direction, as marked by arrows in Fig. 4 (b), a reduction in t_{ch} also produces an increase in $|V_{th}|$, identical to t_{ox} , as shown in Fig. 4 (c). Fig. 4 (c) also indicates that both t_{ch} and t_{ox} are required to be smaller than 5 nm to achieve a $|V_{th}|$ of more than -1.5 V at an Al composition of 18%, for example.

The threshold voltage predicted from Eq. (5) agrees with the simulated V_{th} as shown in Fig. 5 (a) at lower Al mole fraction. The deviation between the two at higher x_b results from a change in the ionized trap density which has been ignored in Eq. (5) for simplicity. A plot of I_{ON}/I_{OFF} against V_{th} , as x_b is varied (Fig. 5 (b)), shows a reduction from over 6 orders of magnitude to less than 1, with a reduction in $|V_{th}|$, indicating the trade-off that exists as the device moves from E-mode to D-mode as explained earlier. Furthermore, the $|I_{ON}|$ also reduces to less than half as the device turns from D-mode to E-mode irrespective of t_{ox} (Fig. 5 (c)), demonstrating the severity of the trade-off between $|I_{ON}|$ and $|V_{th}|$ which places a limit upon the conventional heterostructure in achieving E-mode behavior with large $|I_{ON}|$ and high $|V_{th}|$ in p-channel GaN MOSHFETs.

IV. ANALYSIS OF THE NOVEL HETEROSTRUCTURE P-CHANNEL MOSHIFT (HS2)

The above limitations are addressed here with the alternate heterostructure (HS2), introduced earlier, which employs an additional AlGaIn cap layer, sandwiched between the insulator and the GaN channel layer. The AlGaIn cap introduces a positive polarization charge (σ_{cap}) between cap/channel layer to modulate the electric field within the oxide and the AlGaIn cap, as displayed in the corresponding band diagrams in Fig. 6. If σ_{cap} exceeds a certain value (σ_{crit}), the electric field within the oxide and AlGaIn cap layers reverses its direction, which, unlike in HS1, causes the $|V_{th}|$ to rise with an increase in t_{ox} , as shown Fig. 7.

An increase in x_{cap} also lowers the valence band energy in the GaN channel (Fig. 6), leading to an increase in $|V_{th}|$, irrespective of the t_{ox} , as shown in Fig. 8 (a). The intersection point of all the curves at different t_{ox} represents the critical Al mole fraction in the cap x_{crit} when the electric field within the oxide and cap layers becomes zero, causing $|V_{th}|$ to become

independent of t_{ox} . The expression for σ_{crit} in Fig. 8 (a) also confirms its independence of t_{ox} , which is obtained from the application of Gauss' law at the AlGaIn cap/GaN channel and GaN channel/AlGaIn barrier interfaces. An increase in x_{cap} , however, also suppresses the $|I_{ON}|$ (Fig. 8 (b)), due to an overall reduction in negative polarization charge beneath the gate, leading to a reduction in 2DHG density under the gate. An increase in σ_{cap} at higher x_{cap} can effectively deplete the 2DHG under the gate leading to an improvement in the I_{ON}/I_{OFF} , by 14 orders of magnitude, as shown in Fig. 8 (c).

The simulation results for V_{th} are in close agreement with those predicted by Eq. (6), as shown in Fig. 9 (a). If x_b varies for different values of x_{cap} , in Fig. 9 (b), as indicated by the green arrows, both $|I_{ON}|$ and $|V_{th}|$ can be made to increase simultaneously, thus overcoming the trade-off present with HS1 (Fig. 5 (c)) and even HS2 (Figs. 8 (a), (b)). Fig. 9 (c) shows one such example where x_{cap} varies with x_b as $1.8x_b - 0.25$. In contrast to Fig. 5 (c), $|I_{ON}|$ increases with $|V_{th}|$, reaching a maximum of -60 mA/mm at $|V_{th}|$ of -2.4 V, at an oxide thickness of 6 nm used in these settings.

In Fig. 10, the transfer characteristics obtained from the p-channel MOSHFETs with HS1 and HS2 are compared for different V_{th} . In all the cases, the turn-on for HS1 occurs at smaller V_{GS} than for HS2 with a steeper slope. This is because without the additional AlGaIn cap layer in HS1, the gate can effectively modulate the hole gas density within the GaN channel across the oxide layer. For HS1, due to the trade-off between $|I_{ON}|$ and $|V_{th}|$, the $|I_{ON}|$ declines sharply at large $|V_{th}|$, dropping to 20 mA/mm at a V_{th} of -2.3 V. Moreover, since small x_b is used in HS1 to achieve a large $|V_{th}|$, $|I_{ON}|$ shows a saturation at higher V_{GS} due to the limited density of the 2DHG arising from a small polarization charge. Whereas $|I_{ON}|$ of ~ 50 mA/mm is achieved at V_{th} of -2.3 V for HS2 which is more than double compared with HS1, demonstrating its superior performance over conventional heterostructure at higher $|V_{th}|$.

V. CONCLUSION

We have demonstrated that in p-channel GaN MOSHFETs based upon the conventional heterostructure, a high $|V_{th}|$ comes at the cost of thinner oxide and channel and small Al mole fraction. Moreover, the on-current of the device drops to less than 50% as the device turns from D-mode to E-mode, creating a trade-off between on-current level and threshold voltage. These challenges are overcome with an alternate heterostructure based p-channel MOSHIFT that employs an AlGaIn cap layer. It is demonstrated that by suitably adjusting the Al mole fraction in cap AlGaIn layer, not only can the dependence of V_{th} upon oxide thickness be reversed but also the trade-off observed in conventional heterostructure can be minimized, which should no doubt lead to higher performance than any E-mode p-channel GaN HFETs reported to date.

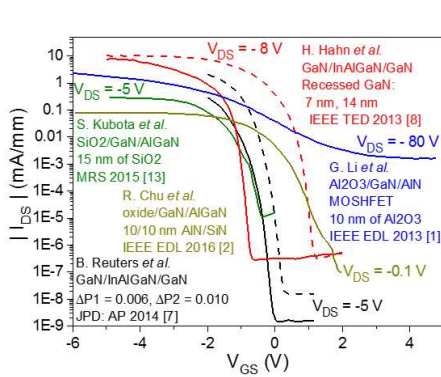


Fig. 1. The transfer characteristics of the state-of-the-art normally-off p-channel HFETs reported to date.

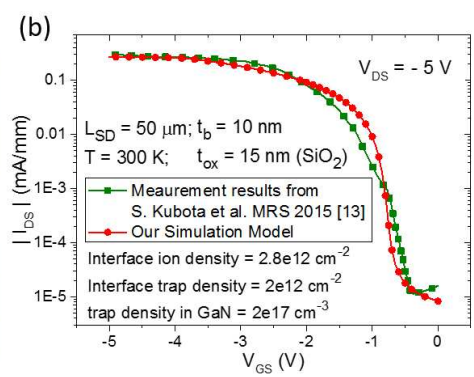
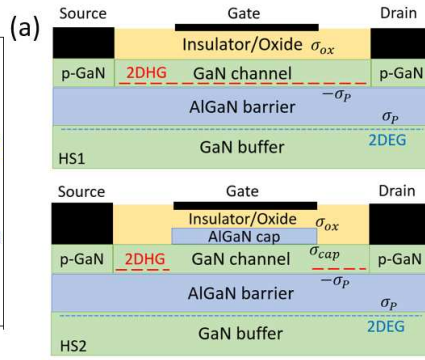


Fig. 2. (a) p-channel GaN MOSHFTs on conventional heterostructure (HS1) and alternate heterostructure (HS2), (b) Verification of our simulation model for HS1 with experiment using Silvaco TCAD [12].

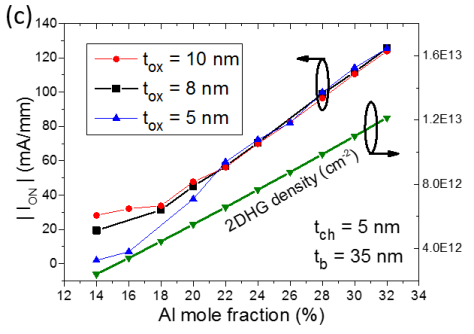
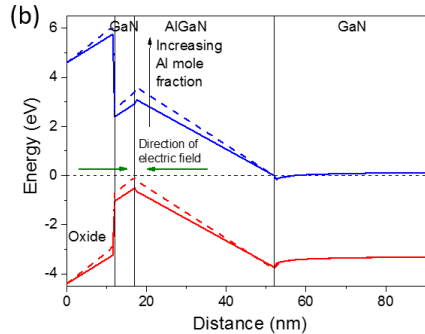
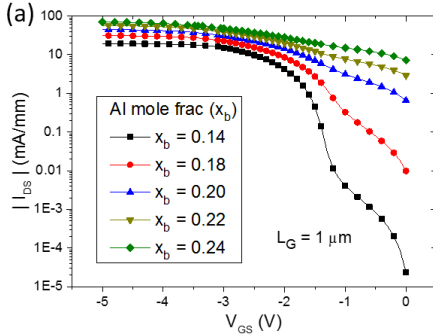


Fig. 3. (a) Comparison of simulated transfer characteristics of HS1 at different Al mole fraction in the barrier layer x_b , (b) Change in the energy band diagram in HS1 beneath the gate with x_b , (c) on-current $|I_{ON}|$ and the density of 2DHG vs. x_b at different oxide (Al_2O_3) thicknesses t_{ox} for HS1.

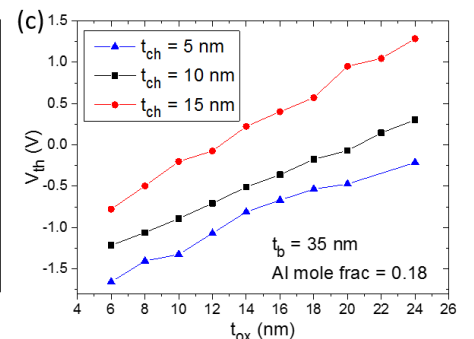
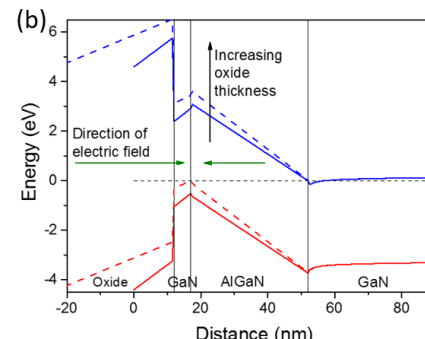
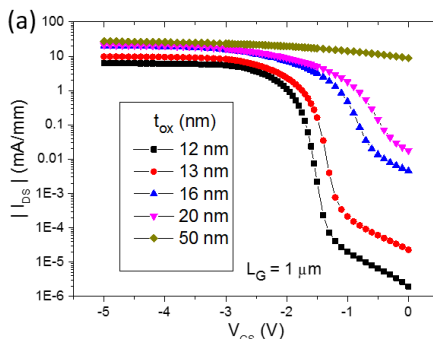


Fig. 4. (a) Comparison of simulated transfer characteristics of HS1 and (b) energy band diagrams beneath the gate at different oxide (Al_2O_3) thicknesses t_{ox} in HS1. (c) Comparison of the threshold voltage V_{th} vs. t_{ox} at different channel thicknesses t_{ch} .

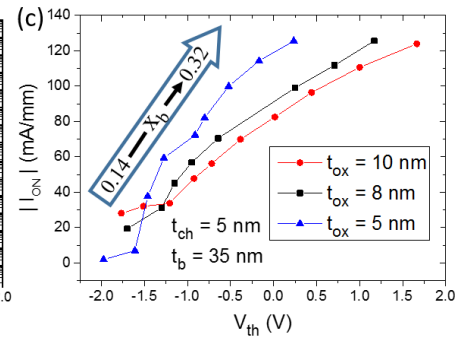
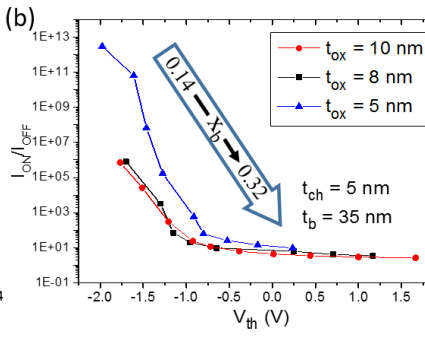
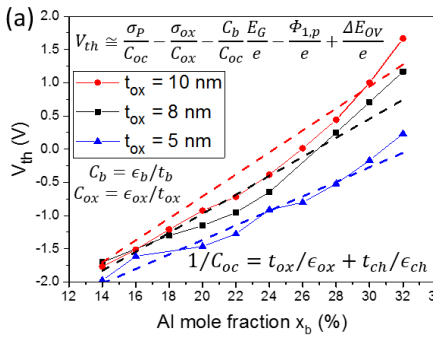


Fig. 5. (a) V_{th} vs. Al mole fraction x_b at different oxide (Al_2O_3) thicknesses t_{ox} , while dashed lines show the V_{th} predictions from Eq. (5). on-off current ratio I_{ON}/I_{OFF} is plotted against V_{th} for HS1 in (b), and $|I_{ON}|$ is plotted against V_{th} in (c) as x_b is varied at different values of t_{ox} . I_{ON}/I_{OFF} improves with a reduction in V_{th} , however the on-current also reduces as the device turns from D-mode to E-mode.

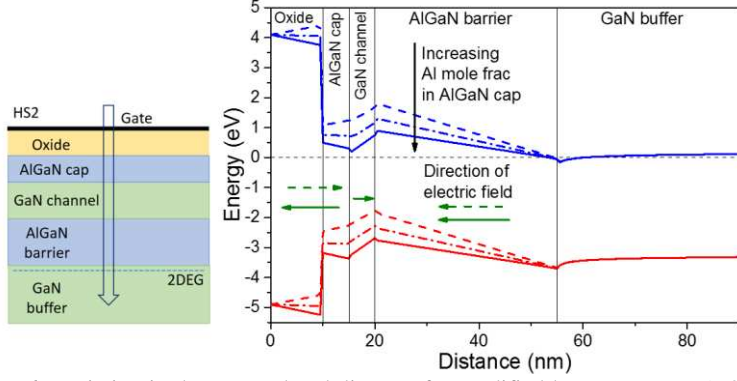


Fig. 6. Variation in the energy band diagram for modified heterostructure (HS2) under the gate with a change in Al mole fractions in AlGaIn cap.

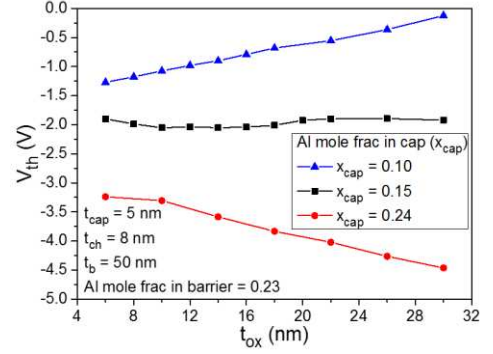


Fig. 7. V_{th} vs. t_{ox} (Al_2O_3) at different Al mole fraction in cap layer x_{cap} . With a rise in x_{cap} , behavior of V_{th} with t_{ox} becomes opposite to that in HS1.

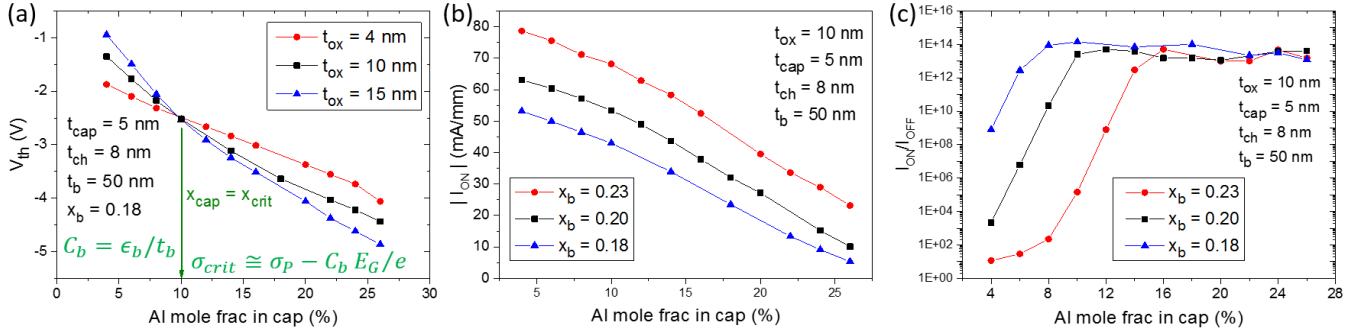


Fig. 8. (a) Comparison of V_{th} vs. Al mole fraction in cap x_{cap} at various oxide (Al_2O_3) thicknesses t_{ox} , in HS2 (b) on-current vs. x_{cap} at different Al mole fraction in AlGaIn barrier layer x_b in HS2, and (c) on-off current ratio with respect to x_{cap} at different x_b in HS2.

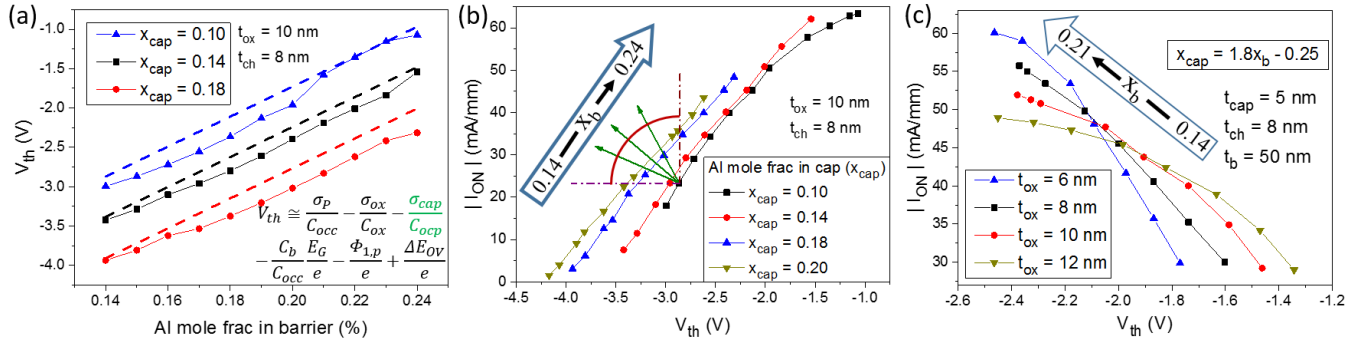


Fig. 9. (a) Comparison of V_{th} vs. Al mole frac. in barrier x_b at different Al mole frac. in cap x_{cap} in HS2, dashed lines are the V_{th} predictions from Eq. (6). (b) $|I_{ON}|$ vs. V_{th} as x_b is varied at different x_{cap} in HS2, green arrows mark the directions along which both $|I_{ON}|$ and $|V_{th}|$ increase, (c) $|I_{ON}|$ vs. V_{th} along one of such directions, where x_{cap} is varied as $1.8x_b - 0.25$, at different Al_2O_3 thicknesses t_{ox} in HS2.

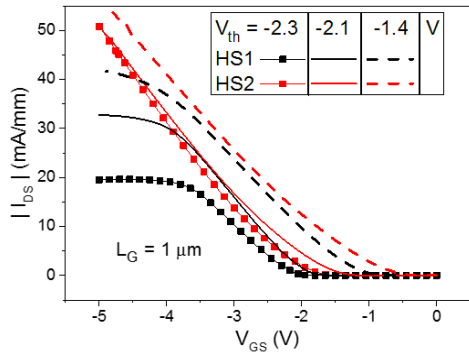


Fig. 10. Comparison of transfer characteristics between two p-channel MOSFETs employing heterostructure 1 (HS1) and heterostructure 2 (HS2).

REFERENCES

- [1] G. Li *et al.*, *IEEE Electron Device Lett.*, vol. 34, no. 7, pp. 852–854, 2013.
- [2] R. Chu, *IEEE Electron Device Lett.*, vol. 37, no. 3, pp. 269–271, 2016.
- [3] A. Nakajima *et al.*, *J. Appl. Phys.*, vol. 115, 2014.
- [4] A. Nakajima *et al.*, *Appl. Phys. Express*, vol. 3, 2010.
- [5] M. S. Shur *et al.*, *Appl. Phys. Lett.*, vol. 76, no. 21, p. 3061, 2000.
- [6] S. Yang *et al.*, *IEEE TED*, vol. 60, no. 10, pp. 3040–3046, 2013.
- [7] B. Reuters *et al.*, *J. Phys. D Appl. Phys.*, vol. 47, p. 175103, 2014.
- [8] H. Hahn *et al.*, *IEEE TED*, vol. 60, no. 10, pp. 3005–3011, 2013.
- [9] F. J. Kub *et al.*, U.S. Patent No. 9,275,998, 2015.
- [10] J. D. Albrecht *et al.*, *J. Appl. Phys.*, vol. 83, no. 9, p. 4777, 1998.
- [11] M. Farahmand *et al.*, *IEEE TED*, vol. 48, no. 3, pp. 535–542, 2001.
- [12] “Silvaco TCAD Atlas.” <http://www.silvaco.co.uk/products/tcad.html>.
- [13] S. Kubota, *et al.*, *Material Research Society*, 2015.
- [14] H. Hahn, Ph.D. thesis, RWTH Aachen University, 2014.